AGU PUBLICATIONS

Geophysical Research Letters

RESEARCH LETTER
10.1002/2014GL061779

**Key Points:**
- We first identified a new feature of knobby terrain on ancient Martian volcanoes
- The knobby terrain is made of fine-grained materials (tephra)
- The knobby terrains indicate a dominant early explosive volcanism

**Supporting Information:**
- Figure S1 and Table S1

**Correspondence to:**
J. Huang,
jhuang.cug@gmail.com

**Citation:**
Huang, J., and L. Xiao (2014), Knobby terrain on ancient volcanoes as an indication of dominant early explosive volcanism on Mars, *Geophys. Res. Lett.*, *41*, 7019–7024, doi:10.1002/2014GL061779.

Received 4 SEP 2014
Accepted 1 OCT 2014
Accepted article online 4 OCT 2014
Published online 24 OCT 2014

# Knobby terrain on ancient volcanoes as an indication of dominant early explosive volcanism on Mars

**Jun Huang[1] and Long Xiao[1]**

[1]Planetary Science Institute, China University of Geosciences, Wuhan, China

**Abstract** Determining if the mechanically weak materials of the upper crust are products of early explosive volcanism or generated by modification of extensive effusive lava flows is important for understanding the geologic and thermal history of Mars. We examined 75 recently identified preserved ancient volcanoes, whose eruption styles are representative of early volcanism. We describe a unique knobby terrain that is associated with 17 of these volcanoes. This newly identified terrain is characterized by a combination of high-resolution images and thermophysical and thermal infrared hyperspectral data. The morphology characteristics of these knobby terrains are similar to terrestrial eroded ignimbrites, and the thermophysical properties indicate that they are composed of unconsolidated fine-grained materials. The spectral analysis indicates that they experienced some aqueous alteration. We explain the knobby terrain associated with these ancient volcanoes as the products of an early explosive volcanic phase in Martian history, followed by subsequent modification of these deposits.

## 1. Introduction

It is critical to understand the physical nature and source of building materials of the upper Martian crust to gain insight into early Martian volcanism. These materials have been recognized as mechanically weak [*Schultz*, 2002; *Stewart and Valiant*, 2006]. A popular view is that effusive volcanism was dominant in the early history of Mars, and subsequent impact events have generated a highly fractured megaregolith from extensive lava flows [e.g., *McEwen et al*., 1999]. An alternate hypothesis is that mechanically weak materials were mainly the products of extensive explosive volcanism and were subsequently modified by geologic processes [e.g., *Bandfield et al*., 2013]. Observations of ancient volcanic features can provide insights into the dominant early eruption style, but most ancient Martian volcanoes were buried by lava from later volcanism or severely modified by subsequent geologic processes. Several ancient central volcanoes located in the Circum-Hellas [*Williams et al*., 2009] and Arabia Terra [*Michalski and Bleacher*, 2013] show strong evidence for explosive eruptions. Recently, 75 globally distributed, preserved ancient volcanoes have been identified by Xiao *et al*., [2012], and they are among the oldest eruption centers identified on the surface of Mars. These ancient volcanoes have been inactive for the majority of Martian geologic history, and they preserve clues of the style of early global volcanic eruption. Here we have identified and characterized knobby terrains associated with 17 out of 75 ancient volcanoes with high-spatial-resolution visible images and thermophysical and thermal infrared hyperspectral data. The best explanation for these features is that they are the eroded remnants of pyroclastic materials, which supports a mechanism of dominant early explosive volcanism on Mars.

## 2. Methods

We used imaging data from the Thermal Emission Imaging System (THEMIS: ~100 m/pixel) [*Christensen et al*., 2004] global mosaic [*Edwards et al*., 2011] and gridded topographic data from the Mars Orbiter Laser Altimeter (MOLA: 128 ppd) [*Smith et al*., 2001] to show the overall regional context. Local albedo and dust cover index (DCI) [*Ruff and Christensen*, 2002] were derived from Thermal Emission Spectrometer (TES: $3 \times 6$ km$^2$ spatial resolution) data [*Christensen et al*., 2001]. We selected 12 high-quality TES spectra (Figure S1 in the supporting information: ock 5980, ick 1371–1374) with minimum surface air fall dust (DCI $> 0.97$) and other constraints similar to the study of *Rogers et al*. [2007], averaged them, and removed the atmospheric components using a linear unmixing method [*Bandfield et al*., 2000a; *Smith et al*., 2000] to analyze the surface emissivity. We then deconvolved the spectrum with the mineral library of *Rogers and Fergason* [2011] between 1301 and 307 cm$^{-1}$

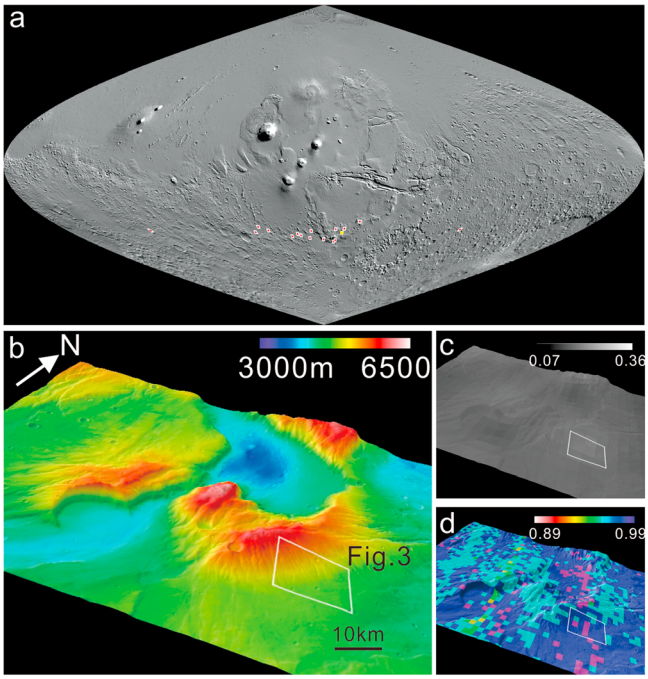


**Figure 1.** (a) Identified knobby terrains on sinusoidal projected MOLA-shaded relief [*Smith et al.*, 1999]. The yellow square labels the location of the volcano in (b). (b) color coded MOLA-gridded elevation (10 times the vertical exaggeration) over THEMIS day IR mosaic [*Edwards et al.*, 2011]. A wind rift cut through this ancient volcano (centered at 272.07°E, 37.8°S) and extensive channels are on the slopes. (c) The DCI map [*Ruff and Christensen*, 2002] on MOLA-shaded relief. The DCI values (0.96–0.99) indicate that the slope is relatively free of dust. (d) The TES albedo [*Christensen et al.*, 2001] on MOLA-shaded relief.

to quantitatively determine the surface mineralogy. In order to decipher the thermophysical nature of the materials in these terrains, we used thermal inertia data derived from THEMIS nighttime infrared (IR) data [*Fergason et al.*, 2006]. Finally, we presented local and detailed geomorphology using Context Camera (CTX: ~6 m/pixel) [*Malin et al.*, 2007] and High Resolution Imaging Science Experiment (HiRISE: ~30 cm/pixel) images [*McEwen et al.*, 2007].

## 3. Results

The locations of the knobby terrains identified with 17 ancient volcanoes are shown in Figure 1a. All the occurrences are within the southern middle latitudes (30–45°S). In this section, we present detailed observations of the knobby terrains on the southern slope of a heavily modified ancient volcano in Thaumasia Highlands as an example. This volcano stands ~3000 m above adjacent terrains (Figure 1b), and it is cut through by a large rift [*Grott et al.*, 2007]. A crater retention age of ~3.94 Ga [*Xiao et al.*, 2012] indicates that the surface is Noachian in age. The slopes of the volcano are incised by channels that vary in width and depth and form a radial pattern, which may indicate erosion by multiple periods of fluvial activity. The albedos of the southeastern slope materials range from 0.17 to 0.19 (Figure 1c), which indicates that these materials are slightly brighter than the dark regions [*Christensen et al.*, 2001] or covered by some amount of air fall dust. However, the DCI values are between 0.96 and 0.99 (Figure 1d), indicating that the surface is relatively free of air fall dust [*Ruff and Christensen*, 2002]. DCI is more reliable than albedo when determining surface dust coverage, as some features (e.g., the White Rock) with higher albedo have minimum air fall dust [*Ruff et al.*, 2001].

The average atmospherically corrected spectrum (KT) is shown with "Surface Type 2"-like [*Bandfield et al.*, 2000b] spectral shapes of northern Acidalia (NA) and Solis Planum (SP) [*Rogers et al.*, 2007] in Figure 2a. The short-wavelength portion of the KT spectrum is an asymmetric "V" shape (Figure 2b), and it is similar to the spectral shapes of NA and SP between ~8 and 12 μm. The long-wavelength portion of the KT spectrum is generally similar to its counterpart of the NA and SP spectra, but it has a slight slope toward longer wavelengths.

The model fit and modeled mineralogy for the KT spectrum are shown in Figure 2b. The fit is generally good with a root-mean-square error of ~0.11%. Feldspar (~36%) is the dominant group of minerals. The high-silica (montmorillonite: ~25%) group is ~31%, and the pyroxene group is ~19%. The major mineral components of KT spectrum are similar to the deconvolution results of the NA and SP spectra [*Rogers and Christensen*, 2007].

The knobby terrain occurs on interchannel slopes, and it has a rough and blocky appearance at CTX resolution (Figure 3a). The rim and bottom of the channels are much smoother, which indicate that these regions are covered by air fall dust. The knobby terrains and areas covered with air fall dust also can be distinguished from thermal inertia data (Figure 3b); the knobby terrain has an elevated thermal inertia varying from ~190 to 210 $Jm^{-2}K^{-1}s^{-1/2}$, while dust-covered channels have lower values of ~120 $Jm^{-2}K^{-1}s^{-1/2}$.

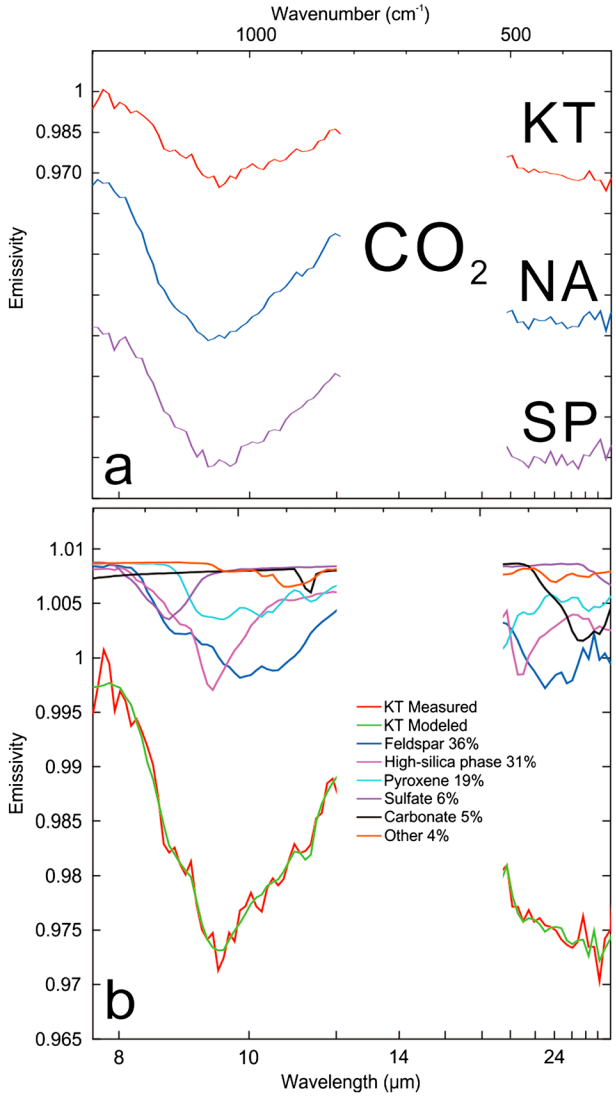


**Figure 2.** Thermal IR spectral characteristics and quantitative mineralogy of the knobby terrain. (a) Averaged and atmospheric corrected TES spectrum of the knobby terrain (KT), the spectra of northern Acidalia (NA), and Solis Planum (SP) [*Rogers et al*., 2007]. (b) Deconvolution of KT spectrum using the mineral library of *Rogers and Fergason* [2011]. The result shows elevated high-silica phase in the materials of the knobby terrain, which is similar to the modeled mineralogy of the NA and SP spectra reported by *Rogers and Christensen* [2007].

The individual knobs are relatively dark toned and are curved near their bases in a style of erosion shown on the slope of our example volcano (Figure 4a) and other ancient volcanoes (Figures 4b and 4c and Table S1 in the supporting information). Their sharp appearances seen in HiRISE images are consistent with the rough surface observed in CTX images (Figure 3a). Individual knobs are separated by topographically low lineations. The lineations are most likely joints occurring in bedrock. Knobs occur in clusters with knobs of similar sizes (Figure 4a), in which larger knobs (~25 m in diameter and ~10 m high) occur in the western half of the image, while smaller knobs (~5–10 m in diameter and ~5 m in height) are seen in the eastern half. What causes knobs to cluster by size is unknown, but it could be related to the differences in material properties, material thickness, or local slope. The knobby material has a sharp appearance and maintains steep slopes, indicating that the material is not loosely deposited. The knobby terrain in this study resembles eroded rhyolitic to dacitic ignimbrites [*Temel et al*., 1998] in Cappadocia, Turkey (Figure 4d).

## 4. Discussion

We suspect that the knobby terrains are distributed more widely than the 17 ancient volcanoes discussed in this study. However, it is difficult to analyze the spatial distribution due to limited data availability: (1) the 21 volcanoes described by *Xiao et al*. [2012] have partial HiRISE coverage, and (2) the derivation of thermal inertia data for surfaces polarward of 45° is challenging [*Fergason et al*., 2006]. We suggest that knobby terrains are blocks made of fine-grained pyroclastic materials based on their morphology and thermophysical properties. The extensive channels on the slope of the volcano indicate that the materials are relatively easy to erode. The typical sharpness and angularity of the knobs are more consistent with the fine-grained deposit than with the blocky rock covered with fine-grained materials, which we would expect to have a smoother, draped-on appearance. The derived thermophysical properties, namely, the thermal inertia, of the knobby terrains support the geomorphologic evidence. Thermal inertia represents a material's resistance to temperature change [*Kieffer et al*., 1977; *Mellon et al*., 2000; *Fergason et al*., 2006] and can be used to determine particle size by assuming that spherical shape particles are homogeneous in both size and composition [*Presley and Christensen*, 1997]. In reality, a qualitative effective particle size can be inferred from the thermal inertia. Previous studies have distinguished different surfaces with relative effective particle sizes [*Fergason et al*., 2006; *Edwards et al*., 2009; *Bandfield et al*., 2013]: rock-dominated regions

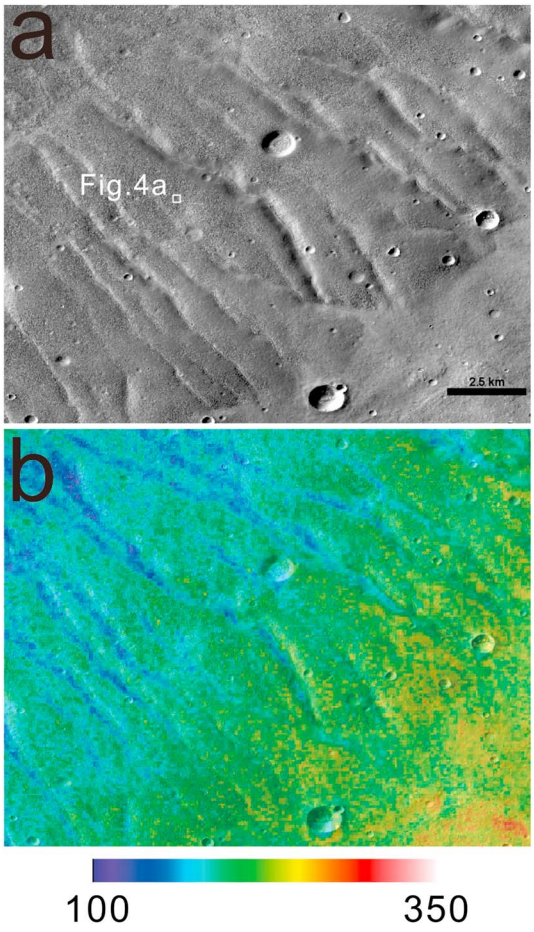


**Figure 3.** Local geomorphology and thermophysical characteristics of the knobby terrain. (a) Tens of channels cut through the volcano's slope. The interchannel region looks rough in the CTX image (ID: B03_010621_1419_XN_38S087W). (b) Color coded thermal inertia derived from THEMIS nighttime IR data (ID: I26494018) on the CTX image. The relatively dust-free knobby terrains (green) are easy to be distinguished from dust cover area (blue).

(>~1200 $Jm^{-2}K^{-1}s^{-1/2}$), coarse-grained materials (~600–1200 $Jm^{-2}K^{-1}s^{-1/2}$), fine-grained materials (~100–600 $Jm^{-2}K^{-1}s^{-1/2}$), and dust-covered areas (<~100 $Jm^{-2}K^{-1}s^{-1/2}$). The knobby terrain is relatively free of air fall dust while the channels are covered by dust, based on DCI values and the appearance in HiRISE scene. Therefore, dust has minimum effects on the qualitative effective particle size of the knob materials, which are possibly made of fine-grained, mechanically weak materials.

The surface spectrum of the knobby terrain provides additional evidence for the possible tephra nature of the knobs. As described above, the spectral shape and deconvolution results are similar to those of the NA and SP spectra [*Rogers and Christensen*, 2007], which indicate elevated abundance of high-silica phase in the materials of the knobs. High-silica phase in TES Surface Type 2-like spectra can be due to either primary volcanic glass [e.g., *Christensen et al*., 2005] or altered high-silica phases such as clays and zeolites [*Wyatt and McSween*, 2002; *Kraft et al*., 2003; *Michalski et al*., 2005], which were discussed in detail by *Rogers and Christensen* [2007]. However, more recent studies have suggested that the Surface Type 2-like spectra tend to indicate the existence of altered minerals [e.g., *Horgan and Bell*, 2012; *Salvatore et al*., 2014]. It is plausible that the finely particulate materials of the knobby terrains with or without a primary volcanic glass reacted with the fluid incising the channels on the volcano slopes. The chemical alteration of explosive volcanic materials has been predicted by *Wilson and Head* [2007] and observed by *Horgan and Bell* [2012]. Our analysis of the knobby terrains is consistent with this scenario.

We propose a possible formation scenario: (1) a pyroclastic flow was emplaced on the slopes and adjacent area; (2) some fluid eroded the pyroclastic deposits preferentially along the preexisting lineations generated by extensive regional tectonic stress or the lineations were erosional to begin with; (3) wind erosion further modified these terrains; and (4) later lava flows covered much of the pyroclastic material in the surrounding area of this volcano, but exposures of knobby terrains were preserved on the slopes.

The knobby terrain identified in this study provides insights to the dominant eruption style of early Martian history. A brief volcanic history of Mars [*Werner*, 2009; *Carr and Head*, 2010; *Xiao et al*., 2012] is as follows: numerous small central volcanoes are globally distributed in the Noachian. As the planet cooled, most of the small volcanoes stopped growing and the central volcanism concentrated in Tharsis, Elysium, and the Circum-Hellas volcanic provinces. Finally, central volcanism only continued in Tharsis. Large portions of ancient volcanoes were buried by later volcanic materials, and the unburied ones also suffered subsequent severe modification [*Xiao et al*., 2012; *Michalski and Bleacher*, 2013]. The fine-grained nature of the knobby terrains observed related to the ancient volcanoes provides a new piece of evidence to suggest dominantly early explosive volcanism. The ancient volcanoes with knobby terrains may represent the globally distributed explosive central volcanoes. They could be the potential central source region of explosive volcanic products, as

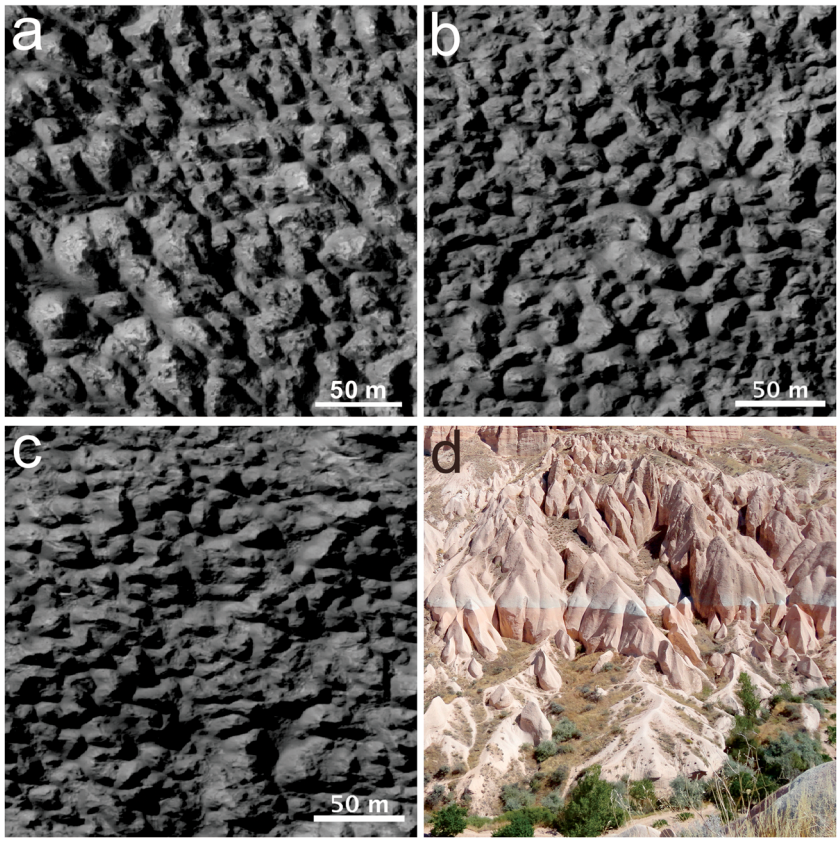


**Figure 4.** A close look at the knobby terrain and its possible counterpart on the Earth. (a) The knobs have different size and sharp appearances in the HiRISE image (ID: PSP_010621_1420). Numerous lineations separated the individual knobs. (b) The knobby terrain identified at 259.644°E, 41.613°S (ID: ESP_016318_1380). (c) The knobby terrain identified at 243.243°E, 39.363°S (ID: ESP_016701_1400). (d) The eroded ignimbrites in Cappadocia, Turkey. The diameters of the individual "knobs" are ~30–50 m.

predicted by *Michalski and Bleacher* [2013] and may have contributed large amounts of fine particles to the upper crust and the widespread layered deposits in equatorial regions.

## 5. Conclusion

We have identified 17 ancient volcanoes with knobby terrains. Based on geomorphologic, thermophysical, and spectral observations, we infer these knobs to be the remnants of fine-grained volcanic materials modified by subsequent erosion and/or tectonism. This supports the notion that explosive volcanism was the dominant eruption style for central volcanoes for the early history of Mars.

**Acknowledgments**

Insightful reviews by Tim Glotch and Jacob Bleacher greatly improved the quality of this paper. Discussions with M. Kraft, P. Christensen, M. Veto, S. Ruff, C. Haberle, R. Smith, and C. Edwards are appreciated. We searched and visualized all the data in JMARS (jmars.asu.edu) and davinci (davinci.asu.edu). Data can be accessed from pds.jpl.nasa.gov with IDs. This project was supported by National Natural Science Foundation of China (41403052, 41373066), China Postdoctoral Science Foundation (2013 M540614), and Postdoctoral International Exchange Project.

The Editor thanks Timothy Glotch and Jacob Bleacher for their assistance in evaluating this paper.

## References

Bandfield, J. L., P. R. Christensen, and M. D. Smith (2000a), Spectral data set factor analysis and end-member recovery: Application to analysis of Martian atmospheric particulates, *J. Geophys. Res.*, *105*(E4), 9573–9587, doi:10.1029/1999JE001094.

Bandfield, J. L., V. E. Hamilton, and P. R. Christensen (2000b), A global view of Martian surface compositions from MGS-TES, *Science*, *287*(5458), 1626–1630.

Bandfield, J. L., C. S. Edwards, D. R. Montgomery, and B. D. Brand (2013), The dual nature of the martian crust: Young lavas and old clastic materials, *Icarus*, *222*(1), 188–199.

Carr, M. H., and J. W. Head (2010), Geologic history of Mars, *Earth Planet. Sci. Lett.*, *294*(3-4), 185–203.

Christensen, P. R., J. L. Bandfield, V. E. Hamilton, D. A. Howard, M. D. Lane, J. L. Piatek, S. W. Ruff, and W. L. Stefanov (2000), A thermal emission spectral library of rock-forming minerals, *J. Geophys. Res.*, *105*(E4), 9735–9739, doi:10.1029/1998JE000624.

Christensen, P. R., et al. (2001), Mars Global Surveyor Thermal Emission Spectrometer experiment: Investigation description and surface science results, *J. Geophys. Res.*, *106*(E10), 23,823–23,871, doi:10.1029/2000JE001370.

Christensen, P. R., et al. (2004), The Thermal Emission Imaging System (THEMIS) for the Mars 2001 Odyssey Mission, *Space Sci. Rev.*, *110*(1–2), 85–130.

Christensen, P. R., et al. (2005), Evidence for magmatic evolution and diversity on Mars from infrared observations, *Nature*, *436*(7050), 504–509, doi:10.1038/nature03639.
Edwards, C. S., J. L. Bandfield, P. R. Christensen, and R. L. Fergason (2009), Global distribution of bedrock exposures on Mars using THEMIS high-resolution thermal inertia, *J. Geophys. Res.*, *114*, E11001, doi:10.1029/2009JE003363.
Edwards, C. S., K. J. Nowicki, P. R. Christensen, J. Hill, N. Gorelick, and K. Murray (2011), Mosaicking of global planetary image data sets: 1. Techniques and data processing for Thermal Emission Imaging System (THEMIS) multi-spectral data, *J. Geophys. Res.*, *116*, E10008, doi:10.1029/2010JE003755.
Fergason, R. L., P. R. Christensen, and H. H. Kieffer (2006), High-resolution thermal inertia derived from the Thermal Emission Imaging System (THEMIS): Thermal model and applications, *J. Geophys. Res.*, *111*, E12004, doi:10.1029/2006JE002735.
Grott, M., P. Kronberg, E. Hauber, and B. Cailleau (2007), Formation of the double rift system in the Thaumasia Highlands, Mars, *J. Geophys. Res.*, *112*, E06006, doi:10.1029/2006JE002800.
Horgan, B., and J. F. Bell (2012), Widespread weathered glass on the surface of Mars, *Geology*, G32755.1, doi:10.1130/G32755.1.
Kieffer, H. H., T. Z. Martin, A. R. Peterfreund, B. M. Jakosky, E. D. Miner, and F. D. Palluconi (1977), Thermal and albedo mapping of Mars during the viking primary mission, *J. Geophys. Res.*, *82*(28), 4249–4291, doi:10.1029/JS082i028p04249.
Kraft, M. D., J. R. Michalski, and T. G. Sharp (2003), Effects of pure silica coatings on thermal emission spectra of basaltic rocks: Considerations for Martian surface mineralogy, *Geophys. Res. Lett.*, *30*(24), 2288, doi:10.1029/2003GL018848.
Malin, M. C., et al. (2007), Context Camera Investigation on board the Mars Reconnaissance Orbiter, *J. Geophys. Res.*, *112*, E05S04, doi:10.1029/2006JE002808.
McEwen, A. S., M. C. Malin, M. H. Carr, and W. K. Hartmann (1999), Voluminous volcanism on early Mars revealed in Valles Marineris, *Nature*, *397*(6720), 584–586.
McEwen, A. S., et al. (2007), Mars Reconnaissance Orbiter's High Resolution Imaging Science Experiment (HiRISE), *J. Geophys. Res.*, *112*, E05S02, doi:10.1029/2005JE002605.
Mellon, M. T., B. M. Jakosky, H. H. Kieffer, and P. R. Christensen (2000), High-resolution thermal inertia mapping from the Mars global surveyor thermal emission spectrometer, *Icarus*, *148*(2), 437–455.
Michalski, J. R., and J. E. Bleacher (2013), Supervolcanoes within an ancient volcanic province in Arabia Terra, Mars, *Nature*, *502*(7469), 47–52.
Michalski, J. R., M. D. Kraft, T. G. Sharp, L. B. Williams, and P. R. Christensen (2005), Mineralogical constraints on the high-silica martian surface component observed by TES, *Icarus*, *174*(1), 161–177.
Presley, M. A., and P. R. Christensen (1997), Thermal conductivity measurements of particulate materials 2. Results, *J. Geophys. Res.*, *102*(E3), 6551–6566, doi:10.1029/96JE03303.
Rogers, A. D., and P. R. Christensen (2007), Surface mineralogy of Martian low-albedo regions from MGS-TES data: Implications for upper crustal evolution and surface alteration, *J. Geophys. Res.*, *112*, E01003, doi:10.1029/2006JE002727.
Rogers, A. D., and R. L. Fergason (2011), Regional-scale stratigraphy of surface units in Tyrrhena and Iapygia Terrae, Mars: Insights into highland crustal evolution and alteration history, *J. Geophys. Res.*, *116*, E08005, doi:10.1029/2010JE003772.
Rogers, A. D., J. L. Bandfield, and P. R. Christensen (2007), Global spectral classification of Martian low-albedo regions with Mars Global Surveyor Thermal Emission Spectrometer (MGS-TES) data, *J. Geophys. Res.*, *112*, E02004, doi:10.1029/2006JE002726.
Ruff, S. W., and P. R. Christensen (2002), Bright and dark regions on Mars: Particle size and mineralogical characteristics based on thermal emission spectrometer data, *J. Geophys. Res.*, *107*(E12), 5119, doi:10.1029/2001JE001580.
Ruff, S. W., P. R. Christensen, R. N. Clark, H. H. Kieffer, M. C. Malin, J. L. Bandfield, B. M. Jakosky, M. D. Lane, M. T. Mellon, and M. A. Presley (2001), Mars' "White Rock" feature lacks evidence of an aqueous origin: Results from Mars global surveyor, *J. Geophys. Res.*, *106*(E10), 23,921–23,927, doi:10.1029/2000JE001329.
Salvatore, M. R., J. F. Mustard, J. W. Head Iii, A. D. Rogers, and R. F. Cooper (2014), The dominance of cold and dry alteration processes on recent Mars, as revealed through pan-spectral orbital analyses, *Earth Planet. Sci. Lett.*, *404*, 261–272.
Schultz, R. A. (2002), Stability of rock slopes in Valles Marineris, Mars, *Geophys. Res. Lett.*, *29*(19), 1932, doi:10.1029/2002GL015728.
Smith, D. E., et al. (1999), The global topography of Mars and implications for surface evolution, *Science*, *284*(5419), 1495–1503.
Smith, D. E., et al. (2001), Mars orbiter laser altimeter: Experiment summary after the first year of global mapping of Mars, *J. Geophys. Res.*, *106*(E10), 23,689–23,722, doi:10.1029/2000JE001364.
Smith, M. D., J. L. Bandfield, and P. R. Christensen (2000), Separation of atmospheric and surface spectral features in Mars global surveyor Thermal Emission Spectrometer (TES) spectra, *J. Geophys. Res.*, *105*(E4), 9589–9607, doi:10.1029/1999JE001105.
Stewart, S. T., and G. J. Valiant (2006), Martian subsurface properties and crater formation processes inferred from fresh impact crater geometries, *Meteorit. Planet. Sci.*, *41*(10), 1509–1537.
Temel, A., M. N. Gündoğdu, A. Gourgaud, and J.-L. Le Pennec (1998), Ignimbrites of Cappadocia (Central Anatolia, Turkey): Petrology and geochemistry, *J. Volcanol. Geotherm. Res.*, *85*(1–4), 447–471.
Werner, S. C. (2009), The global martian volcanic evolutionary history, *Icarus*, *201*(1), 44–68.
Williams, D. A., et al. (2009), The Circum-Hellas Volcanic Province, Mars: Overview, *Planet. Space Sci.*, *57*(8-9), 895–916.
Wilson, L., and J. W. Head (2007), Explosive volcanic eruptions on Mars: Tephra and accretionary lapilli formation, dispersal and recognition in the geologic record, *J. Volcanol. Geotherm. Res.*, *163*(1–4), 83–97.
Wyatt, M. B., and H. Y. McSween (2002), Spectral evidence for weathered basalt as an alternative to andesite in the northern lowlands of Mars, *Nature*, *417*(6886), 263–266.
Xiao, L., J. Huang, P. R. Christensen, R. Greeley, D. A. Williams, J. Zhao, and Q. He (2012), Ancient volcanism and its implication for thermal evolution of Mars, *Earth Planet. Sci. Lett.*, *323–324*, 9–18.